Available online at www.sciencedirect.com

ScienceDirect

Energy Procedia 38 (2013) 94 – 100

Energy Procedia

SiliconPV: March 25-27, 2013, Hamelin, Germany

Calibration of electrochemical capacitance-voltage method on pyramid texture surface using scanning electron microscopy

Yuji Komatsu[a,*], Daisuke Harata[a,b], Erik W. Schuring[c], Ard H.G. Vlooswijk[d], Shigetaka Katori[e], Shizuo Fujita[e], Peter R. Venema[d], Ilkay Cesar[a]

[a]*ECN Solar Energy, P.O.Box 1, 1755ZG Petten, the Netherlands*
[b]*Department of Electronic Science and Engineering, Kyoto University, Nishikyo-ku, Kyoto 615-8530, Japan*
[c]*ECN Environment & Energy Engineering, P.O.Box 1, 1755ZG Petten, the Netherlands*
[d]*Tempress Systems BV, Radeweg 31, 8171MD Vaassen, the Netherlands*
[e]*Photonics and Electronics Science and Engineering Center, Kyoto University, Nishikyo-ku, Kyoto 615-8530, Japan*

Abstract

The electrochemical capacitance-voltage (ECV) technique can practically profile carrier concentrations on textured surfaces, but reliable calibration of the surface area is strongly demanded since it plays a decisive role in calculating both the carrier concentration and the profiling depth. In this work, we calibrate the area factor of pyramidally textured surfaces by comparing ECV profiles with cross-sectional scanning electron microscopy image, and found out it is 1.66, and not 1.73 which was formerly assumed. Furthermore, the calibrated area factor was applied to $POCl_3$ and BBr_3 diffusions which resulted in comparable diffusion profiles for both textured and polished surfaces.

Keywords: ECV; doping profile; texture; pyramid; SEM; BBr_3; $POCl_3$

1. Introduction

The electrochemical capacitance-voltage (ECV) [1,2] method is commonly used in profiling the surface doping concentration of silicon solar cells [3,4] due to its reasonable cost of the measurement equipment and the increasing reliability achieved by the effort of the equipment suppliers. While secondary ion mass spectroscopy (SIMS) has difficulty in characterizing textured wafers, ECV can practically measure them by assuming the area factor ([surface area] / [projected area]) is known.

---

* Corresponding author. Tel.: +31-224-56-4303; fax: +31-224-56-8214.
E-mail address: komatsu@ecn.nl.

doi:10.1016/j.egypro.2013.07.254

However, many publications still report the results measured on polished wafers as the reference for textured wafers. The textured wafers got the doping process simultaneously with the reference and will be processed to completed solar cells. This is almost the same procedure when SIMS is employed [5] with which the depth calibration on textured wafers is quite challenging. In other publications, there is no clear statement on the area factor though the description implies the measurement was carried out using textured wafers. It is probably due to the lack of evidence which proves the reliability of the area factor.

So far, Bock *et al.* used 1.73 as the area factor for pyramidally textured surfaces and calibrated with the sheet resistance measured by 4 point probes [3], assuming the validity of the SEMI standard table [6] which correlates the resistivity of silicon with the carrier concentration even for highly doped textured surface. WEP, an ECV equipment supplier, also recommends the use of 1.73 (or 1.7, considering the effective digits) for pyramidally textured surfaces in its operation manual [7], and instructs a practical calibration by using a textured wafer with known resistivity before getting diffusion. The accuracy of this calibration is not well insured because it depends on the depletion layer thickness during the capacitance-voltage (C-V) measurements. Due to the base doping, it can be as thick as 0.3 μm which is of the ~10% range of the texture geometry when a typical solar cell wafer is used.

Heinrich *et al.* measured the ECV profiles of laser-doped multicrystalline surfaces using the area factor obtained by 3-dimensional confocal microscope [4]. This method relies on the definition of a data-smoothing procedure since the acquired data include a lot of scattered noise which makes it difficult to define a 3D geometry, especially for textured surfaces. The equipment has a potential difficulty in accurate definition of textured solar cell surfaces because it employs the reflection of perpendicular light beam as the probe while the textured surface is designed to prevent such reflection itself.

In this study, we employ cross sectional observation for the calibration of ECV using scanning electron microscopy (SEM) imaging. Several reports in literature state that a highly doped p^+-Si layer has a larger secondary electron yield than a less doped substrate when a cleaved surface is observed using SEM [8-10]. We compare ECV doping profiles with the cross sectional observation of the p^+-doped layer for both polished and pyramidally textured surfaces to calibrate the area factor. In addition, we verify the calibration by comparing the ECV profiles between polished and textured surfaces which are processed with $POCl_3$ or BBr_3 tube furnace diffusion simultaneously.

2. Experiment

ECV calculates the surface carrier concentration of semiconductors from the C-V measurement of the quasi-Schottky junction which is formed with the electrolyte [1] that is NH_4HF_2 in case of silicon [2,7]. The electrolyte also intermediates electrochemical etching, and the etched depth can be calculated from the integrated charge of the etching current. By repeating C-V measurement and etching alternately, ECV enables to clarify the depth profile of the electrically active carrier concentration near the surface. The carrier concentration N is calculated as:

$$N = \frac{-2}{q\varepsilon_r\varepsilon_0 A^2 \dfrac{d(1/C^2)}{dV}} , \tag{1}$$

where, q is the unit charge of electron; ε_r is the relative permittivity; ε_0 is the permittivity of vacuum; A is the area of the measurement spot; C is the capacitance; and V is the bias voltage. The profiling depth x is:

$$x = x_{\mathrm{etc}} + w_{\mathrm{dep}} = \frac{Q}{qn_V}\cdot\frac{M_{mol}}{\rho\, N_A}\cdot\frac{1}{A} \quad + \quad \varepsilon_r\varepsilon_0 A\sqrt{\left|(V - V_{\mathrm{fb}})\cdot\frac{d(1/C^2)}{dV}\right|} , \tag{2}$$

where, x_{etc} is the etched depth; w_{dep} is the depletion layer thickness; Q is the total charge derived from integration of the etching current; n_V is the number of effective valence electrons; M_{mol} is the mass of 1

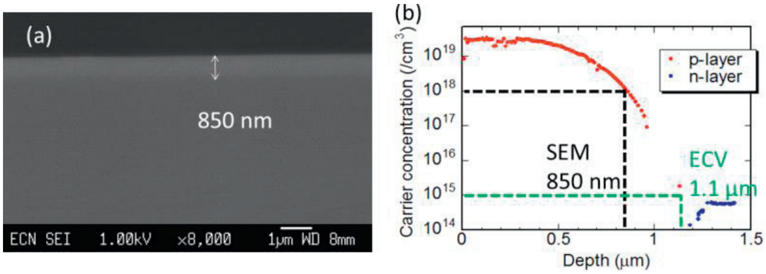

Fig.1. Characterization of a boron-diffused layer on an n-type wafer with a polished surface by (a) cross sectional SEM; (b) ECV.

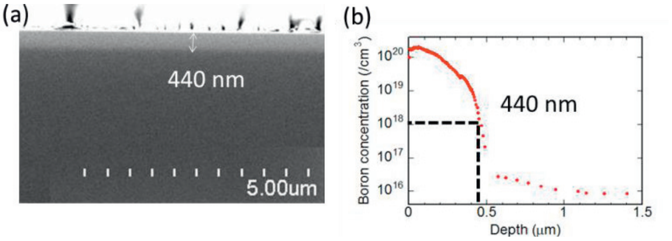

Fig. 2. Characterization of a boron-diffused layer on a p-type wafer with a polished surface by (a) cross sectional SEM; (b) ECV.

mol; ρ is the density; N_A is the Avogadro constant; and V_{fb} is the flat band voltage of the junction. As seen in equations (1) and (2), the measurement spot area A plays a decisive role in the determination of the dopant profile. WEP CVP21 is employed for ECV profiling with the diameter of 0.357 cm for the measurement ring corresponding to 0.100 cm^2 for A.

We evaluated mono crystalline silicon because a cross section for SEM imaging can easily be prepared by cleavage on a (011) plane. For highly doped p^+-Si layer which appears as brighter contrast than lightly-doped base of the wafer, we used BBr_3 diffusion to prepare samples with a p^+-Si layer on top. JEOL JSM-6330F and Hitachi SU-70 were employed for SEM observation, and the accelerating voltage of the electron beam was fixed at 1.0 kV in this work.

3. Results and discussion

3.1. Polished surface

Figure 1(a) shows a cross sectional SEM image of a boron-diffused layer on an n-type wafer with a polished surface and (b) shows its doping profile measured by ECV. The final etched depth of ECV is calibrated by Veeco Dektak 8. Although the p-layer depth is indicated as 1.1 μm by ECV, the bright layer thickness observed by SEM indicates 850 nm where the ECV indicates $N \cong 1.0\times10^{18}$ cm^{-3}. Figure 2(a) and (b) are a SEM image and an ECV profile for a boron-diffusion performed on a p-type wafer. Here, the contrast difference is observed at a depth of 440 nm where $N \cong 1.0\times10^{18}$ cm^{-3}, which confirms the contrast difference appearing at the p^+p border where $N \cong 1.0\times10^{18}$ cm^{-3} and not at the actual pn-junction. This is even favourable because ECV profiling is not good at exactly determining the pn-junction border due to the complicated physics of over 100 nm depletion layer formation caused by both of the quasi- Schottky junction and the pn-junction. Meanwhile, the $[1/C^2–V]$ curve looks straight enough to obtain tangible $d(1/C^2)/dV$ when $N \approx 1.0\times10^{18}$ cm^{-3} where the depletion layer is as thick as 10 nm.

3.2. Textured surface

While SEM observations focus on microscopic areas, ECV evaluates the sample in a macroscopic way. In the case of a polished surface, the microscopic features of an area observed using SEM can be assumed

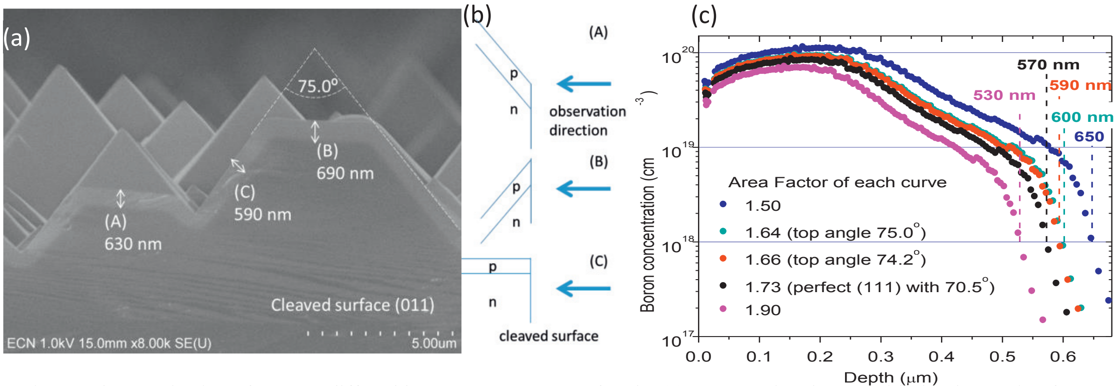

Fig. 3. Characterization of a boron-diffused layer on a textured surface by (a) cross sectional SEM with (b) observation for a textured surface and (c) ECV profiles calculated assuming area factors are 1.50, 1.64, 1.66, 1.73, and 1.90. 1.64 corresponds to pyramid with the top angle as 75.0º, 1.66 as 74.2º, and 1.73 as 70.5º with perfect (111) plane as the micro triangle.

to extend over a macroscopic region even covering the larger ECV measurement spot. But for textured surfaces, several questions arise whether the microscopic and macroscopic features are similar, such as, (i) whether diffusion takes place in the same way either on a facet, at a peak, or in a valley; (ii) whether the depletion layer thickness which determines the capacitance is uniform throughout the ECV measurement spot; (iii) whether electrochemical etching takes place uniformly; (iv) whether the contrast border in the SEM image appears similarly at $N \cong 1.0\times10^{18}$ cm^{-3} as discussed in the previous section, etc.

Figure 3(a) shows a cross-sectional SEM image of a boron-diffused surface with pyramid texture whose size is typical for commercial solar cells. 590-690 nm thickness of the p$^+$-doped layer can be observed brightly at the top, while the pyramid size is at the range of 3-8 μm. The top angle is 75.0º which is larger than 70.5º when the micro facet is a perfect (111) plane. It is also reported by Baker-Finch *et al.* [11] that it is closer to 76º-80º than the commonly accepted value 70.5º.

With respect to the microscopic features, it is still difficult to answer questions (i-iii) mentioned above. But the large difference is observed in the sizes among the texture geometry, the diffused layer depth, and the atomic order where these phenomena take place. Though peaks and valleys may have some influence on the uniformity, the influence will presumably be overwhelmed by the macroscopic ECV measurement.

Regarding question (iv), the diffused layer at point (C) in Fig. 3(a) is perpendicular to the cleaved surface as shown in Fig. 3(b), but those at (A) and (B) are not. This means the contrast difference at point (C) appears because of the same physical effect as the secondary electron emission from polished surfaces observed in Figs. 1(a) and 2(a). Therefore, the contrast difference should appear at $N \cong 1.0\times10^{18}$ cm^{-3} as well. Wager *et al.* attempted 2D doping profiling of textured surface [12], but the physics of the secondary electron emission must be carefully investigated considering the geometry difference among points (A), (B), and (C) in Fig. 3(b). It will be even more complicated for non-pyramid texture.

ECV measurement on a textured surface is practically possible, but considering equations (1) and (2), the area A should be described as:

$$A = FA', \tag{3}$$

where F is the area factor of the textured surface and A' is the measurement spot area. In case of pyramid texture, using microscopic area factor F_μ whose top angle is θ, it can be described as:

$$F = \frac{1}{A'}\sum F_\mu A'_\mu = \frac{1}{A'}\sum \frac{A'_\mu}{\cos(90° - \theta°/2)}, \tag{4}$$

assuming the micro triangle plane is perfectly flat, where A'_μ is the projected area of the micro triangle.

Figure 3(c) shows the calculated curves of ECV profiling from the same sample as is presented in Fig. 3(a), with assuming F as 1.5, 1.64, 1.66, 1.73, and 1.9. 1.64 is for θ = 75.0º and 1.73 corresponds to $\sqrt{3}$ for perfect (111) plane as the triangle with θ = 70.5º. The bright layer thickness at point (C) in Fig. 3(a)

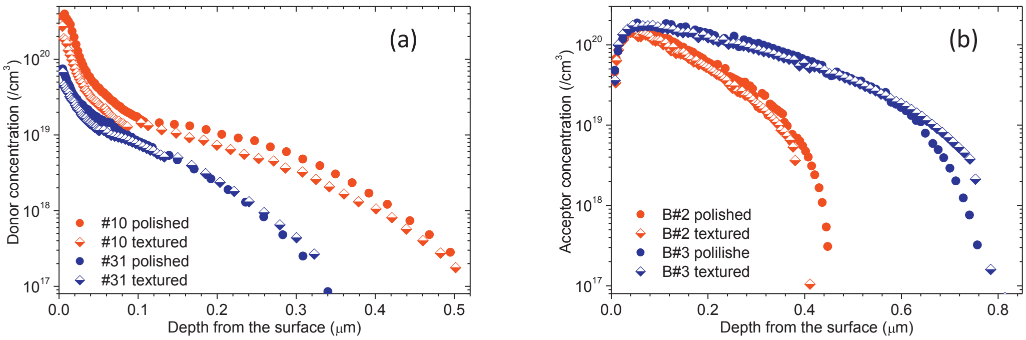

Fig. 4. Examples ECV profiles of (a) 2 $POCl_3$ runs and (b) 2 BBr_3 runs, where 1.66 is employed as area factor for textured surface.

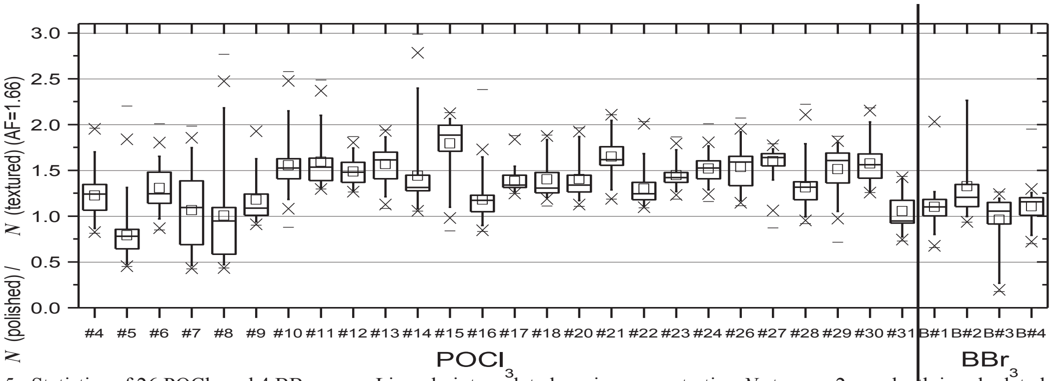

Fig. 5. Statistics of 26 $POCl_3$ and 4 BBr_3 runs. Linearly interpolated carrier concentration N at every 2-nm depth is calculated and N for polish is divided by N for texture at each depth when both $N > 3\times10^{17}\mathrm{cm}^{-3}$. Each box plot represents 25-75% with median, whisker for 5-95%, a small square for average, "X" for 1 and 99%, and "-" for minimum and maximum.

which is at a depth of 590 nm coincides well with the ECV profiling depth assuming F as 1.66 corresponding to $\theta = 74.2°$. This is closer to 1.64 rather than 1.73 which is formerly assumed [3,7], and reflecting the geometry observed using SEM pretty faithfully. The top angle may be a few degrees different from 75.0° when the texturing batch is different, but the result suggests the area factor calculated from the top angle of the pyramids will be pretty close to that for ECV and practically usable for the profile calculation.

3.3. Application and statistical verification of calibrated area factor

As mentioned in section 1, polished wafers are often used as the reference for textured wafers which got the doping process simultaneously. These doping profiles can be now directly compared using the calibrated area factor of 1.66. We carried out 26 different $POCl_3$ diffusion runs and 4 different BBr_3 diffusion runs followed by ECV measurement of both pyramidally textured and polished surfaces. An industry-scale $POCl_3$ and BBr_3 tube furnace Tempress TS81103 was used for diffusion [5,13]. In each diffusion run, the textured and the polished wafers are placed face to face with a gap of 4.6 mm, and the ECV measurement spots were chosen so as both of the spots are also facing each other. With such sample preparation, the two ECV measurement spots of polished and textured surfaces should have nearly identical vapour condition with the same temperature history, and they are likely to have the same doping profiles in most cases.

Figure 4 shows example ECV profiles of (a) 2 $POCl_3$ runs and (b) 2 BBr_3 runs where 1.66 is employed as the area factor for the textured surface. In each case, 2 profile curves of polished and textured are pretty close to each other.

To verify the application numerically and statistically, linearly interpolated carrier concentrations (*N*) at every 2-nm depth are calculated for each profile curve. Then, the deviation ratio (*N*(polished) / *N*(textured)) at each depth is calculated by dividing *N* for polished by *N* for textured in case both *N* values are larger than 3×10^{17} cm^{-3}. Figure 5 shows the statistics of the deviation ratio of the 30 diffusion runs. Overall, the averages of the ratio are almost in the range of 1.0–1.5, and 25–75% ranges are within 0.7–2.0. BBr_3 groups show smaller deviation probably because the SEM calibration was carried out by boron-diffused wafers. But the application to $POCl_3$ also shows that the deviation is within an acceptable level, considering the red curve in Fig. 4(a) is $POCl_3$ #10 in Fig. 5 whose median deviation ratio is 1.5.

In this way, the application of the calibrated area factor 1.66 was evaluated for pyramidally textured surfaces for ECV measurement and resulted in comparable diffusion profiles as for the polished ones. This suggests that potential bottlenecks as described in section 3.2 (questions i-iii) are not limiting the quality of our procedure. The result also supports the wide use of polished wafers as the reference for doping profile of textured wafers by tube furnace diffusion.

4. Conclusion

ECV profiling and cross-sectional SEM imaging were compared using boron-diffused p^+-Si layers. For polished surfaces, contrast difference was found to appear between p^+- and p- layers at $N \cong 1.0\times10^{18}$ cm^{-3}. For pyramid textured surfaces, the area factor *F* was fitted in such a way that the depth at $N \cong 1.0\times10^{18}$ cm^{-3} profiled by ECV should be equivalent to that of the contrast difference in the SEM image. The fitting resulted in $F = 1.66$ which corresponds to the top angle of 74.2º that is close to 75.0º in the same SEM image, and not 1.73 which used to be assumed. Furthermore, the calibrated area factor was applied to tube furnace diffusions of 26 different $POCl_3$ runs and 4 different BBr_3 runs which resulted in comparable diffusion profiles for both textured and polished surfaces.

References

[1] Ambridge T, Faktor MM. Electrochemical capacitance characterization of n-type gallium arsenide. *J Appl Electrochem* 1974;**4**:135-142.

[2] Peiner E, Schlachetzki A, Kruger D. Doping profile analysis in Si by electrochemical capacitance-voltage measurements. *J Electrochem Soc* 1995;**142**:576-580.

[3] Bock R, Altermatt PP, Schmidt J. Accurate extraction of doping profiles from electrochemical capacitance voltage measurements. *Proc of 23rd EU-PVSEC* 2008;**23**:1510-1513.

[4] Heinrich M, Hidayat H, Hameiri Z, Hoex B, Aberle AG. Dopant profiles of laser-doped multicrystalline silicon wafers from electrochemical capacitance-voltage measurements. Proc of 27th *EU-PVSEC* 2012;**27**:1285-1288.

[5] Komatsu Y, Koorn M, Vlooswijk AHG, Venema PR, Stassen AF. Efficiency improvement by deeper emitter with lower sheet resistance for uniform emitters. *Energy Procedia* 2011;**8**:515-520.

[6] Thurber WR, Mattis RL, Liu YM, Filliben JJ. The relationship between resistivity and dopant density for phosphorus-and boron-doped silicon. *National bureau of standards special publication 400-64* 1981; Page 34 and Page 40.

[7] User Manual, Wafer Profiler CPV21, revision 2011. Furtwangen im Schwarzwald: WEP; 2011.

[8] Venables D, Jain H, Collins DC. Secondary electron imaging as a two-dimensional dopant profiling technique: Review and update. *J Vac Sci Technol B* 1998;**16**:362-366.

[9] Elliott SL, Broom RF, Humphreys CJ. Dopant profiling with the scanning electron microscope—A study of Si, *J Appl Phys* 2002;**91**:9116-9122.

[10] El-Gomati M, Zaggout F, Jayacody H, Tear S, Wilson K. Why is it possible to detect doped regions of semiconductors in low voltage SEM: A review and update. *Surf Interface Anal* 2005;**37**:901 – 911.

[11] Baker-Finch SC, McIntosh KR, Reflection distributions of textured monocrystalline silicon: implications for silicon solar cells, *Prog in Photovolt: Res & Appl* 2012; DOI: 10.1002/pip.2186.

[12] Wagner H, Steingrube S, Wolpensinger B, Dastgheib-Shirazi A, Chen R, Dunham ST, Altermatt PP. Analyzing emitter dopant inhomogeneities at textured Si surfaces by using 3D process and device simulations in combination with SEM imaging. *Proc of 38th IEEE-PVSC* 2012;**38**:313-316.

[13] Komatsu Y, Mihailetchi VD, Geerligs LJ, Van Dijk B, Rem JB, Harris M. Homogeneous p^+ emitter diffused using boron tribromide for record 16.4% screen-printed large area n-type mc-Si solar cell. *Sol Ener Mater & Sol Cells* 2009;**93**: 750-752.